Prismatic Delta Robot: A Lagrangian Approach

# Prismatic Delta Robot: A Lagrangian Approach

employed to the delta robot with prismatic actuators. This paper is aimed at covering this literature lack.

## 2 The prismatic Delta robot

The architecture of the delta robot with prismatic joints is depicted in Fig.1. The robot is a parallel machine composed by a platform and three legs each of them is a serial kinematic chain of type $P(SS)_2$. Due to the presence of the parallelograms in each leg, the platform can only translate along the three directions. The prismatic actuated joints are vertical and connect the three carts to the fixed basement. Points $A_1$, $A_2$ and $A_3$ are defined in the middle of the short sides of the parallelograms in correspondence of the carts, while points $P_1$, $P_2$ and $P_3$ are defined in the middle of the opposite sides, in correspondence of the platform. Points $B_1$, $B_2$ and $B_3$ are the vertical projections of points $A_1$, $A_2$ and $A_3$ on the basement plane. A fixed reference system OXYZ is located in the center of the basement, with X axis parallel to segment $B_1B_2$ and oriented from $B_1$ to $B_2$ and Y axis oriented towards point $B_3$. Both triplets $B_1B_2B_3$ and $P_1P_2P_3$ identify equilateral triangles attached to the basement and to the platform respectively. The side lengths of these triangles are indicated as $s_B$ (triangle on basement) and $s_P$ (triangle on platform). Point P is located in the center of the platform.

The dofs associated to the prismatic joints are indicated with $q_1$, $q_2$ and $q_3$ and represent the coordinates along Z axis of points $A_1$, $A_2$ and $A_3$ respect to fixed reference frame.

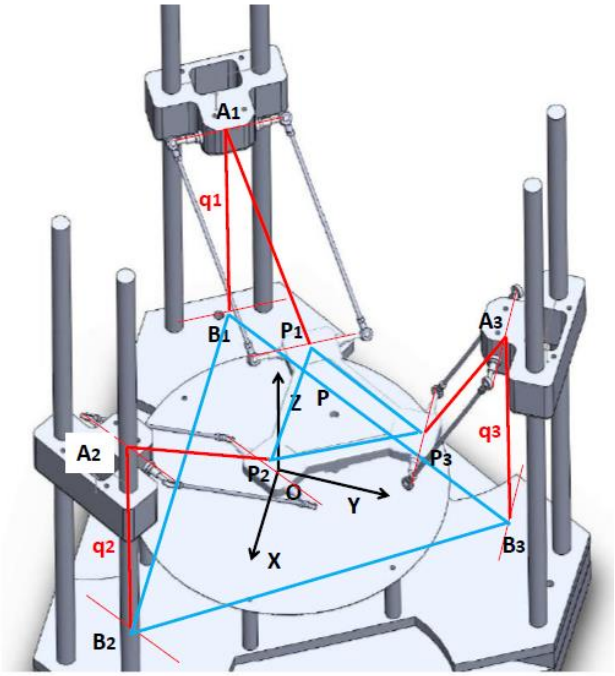


**Fig. 1.** Architecture of the prismatic Delta robot

# 3 Kinematics

The direct kinematics study involves the calculation of position, velocity and acceleration of the platform when the input trajectories in prismatic joints are known. Vice versa, the inverse kinematics involves the calculation of the joints trajectories when the motion of the platform is supposed to be known.

The closure equations are the following:

$$\begin{aligned} \boldsymbol{OB}_1 + \boldsymbol{B}_1\boldsymbol{A}_1 + \boldsymbol{A}_1\boldsymbol{P}_1 + \boldsymbol{P}_1\boldsymbol{P} = \boldsymbol{OP} \\ \boldsymbol{OB}_2 + \boldsymbol{B}_2\boldsymbol{A}_2 + \boldsymbol{A}_2\boldsymbol{P}_2 + \boldsymbol{P}_2\boldsymbol{P} = \boldsymbol{OP} \\ \boldsymbol{OB}_3 + \boldsymbol{B}_3\boldsymbol{A}_3 + \boldsymbol{A}_3\boldsymbol{P}_3 + \boldsymbol{P}_3\boldsymbol{P} = \boldsymbol{OP} \end{aligned} \tag{1}$$

Imposing that the length of segments $\boldsymbol{A}_1\boldsymbol{P}_1$, $\boldsymbol{A}_2\boldsymbol{P}_2$ and $\boldsymbol{A}_3\boldsymbol{P}_3$ is constant in time and equal to *l*, the length of the long side of the parallelograms, the following non-linear equations are derived:

$$\begin{aligned} \left(x_P + \frac{S_B}{2} - \frac{S_P}{2}\right)^2 + \left(y_P + \frac{S_B}{2\sqrt{3}} - \frac{S_P}{2\sqrt{3}}\right)^2 + (z_P - q_1)^2 = l^2 \\ \left(x_P - \frac{S_B}{2} + \frac{S_P}{2}\right)^2 + \left(y_P + \frac{S_B}{2\sqrt{3}} - \frac{S_P}{2\sqrt{3}}\right)^2 + (z_P - q_2)^2 = l^2 \\ {x_P}^2 + \left(y_P - \frac{S_B}{\sqrt{3}} + \frac{S_P}{\sqrt{3}}\right)^2 + (z_P - q_3)^2 = l^2 \end{aligned} \tag{2}$$

## 3.1 Direct kinematics

Known $q_1$, $q_2$ and $q_3$ and their first and second time derivatives, the direct kinematics allows to compute the coordinates $x_P$, $y_P$ and $z_P$ of point P and their time derivatives. As system (2) is non-linear, it can be solved with an iterative method such as Newton Raphson or the three spheres intersection algorithm [6].

The velocities are easily computed solving a linear system resulting from the differentiation of system (2). These equations can be written in a more compact way using the matrix notation:

$$J_x \begin{Bmatrix} \dot{x}_P \\ \dot{y}_P \\ \dot{z}_P \end{Bmatrix} = J_q \begin{Bmatrix} \dot{q}_1 \\ \dot{q}_2 \\ \dot{q}_3 \end{Bmatrix} \tag{3}$$

where $J_x$ and $J_q$ are the Jacobian matrixes. It results

$$\begin{Bmatrix} \dot{x}_P \\ \dot{y}_P \\ \dot{z}_P \end{Bmatrix} = J_x^{-1} J_q \begin{Bmatrix} \dot{q}_1 \\ \dot{q}_2 \\ \dot{q}_3 \end{Bmatrix} \tag{4}$$

The accelerations are obtained differentiating once more equations system (4) and expressing in matrix notation. It results

$$\begin{Bmatrix}\ddot{x}_P\\ \ddot{y}_P\\ \ddot{z}_P\end{Bmatrix} = J_x^{-1}\left(J_q\begin{Bmatrix}\ddot{q}_1\\ \ddot{q}_2\\ \ddot{q}_3\end{Bmatrix} - \begin{Bmatrix}\dot{x}_P^2+\dot{y}_P^2+(\dot{z}_P-\dot{q}_1)^2\\ \dot{x}_P^2+\dot{y}_P^2+(\dot{z}_P-\dot{q}_2)^2\\ \dot{x}_P^2+\dot{y}_P^2+(\dot{z}_P-\dot{q}_3)^2\end{Bmatrix}\right) \tag{5}$$

### 3.2 Inverse kinematics

The inverse problem is simpler, as the joint parameters $q_1$, $q_2$ and $q_3$ can be expressed in explicit way as a function of the platform coordinates:

$$\begin{aligned} q_1 &= z_P \pm \sqrt{l^2-\left(x_P+\frac{S_B}{2}-\frac{S_P}{2}\right)^2-\left(y_P+\frac{S_B}{2\sqrt{3}}-\frac{S_P}{2\sqrt{3}}\right)^2}\\ q_2 &= z_P \pm \sqrt{l^2-\left(x_P-\frac{S_B}{2}+\frac{S_P}{2}\right)^2-\left(y_P+\frac{S_B}{2\sqrt{3}}-\frac{S_P}{2\sqrt{3}}\right)^2}\\ q_3 &= z_P \pm \sqrt{l^2-{x_P}^2-\left(y_P-\frac{S_B}{\sqrt{3}}+\frac{S_P}{\sqrt{3}}\right)^2} \end{aligned} \tag{6}$$

The velocities are computed solving system

$$\begin{Bmatrix}\dot{q}_1\\ \dot{q}_2\\ \dot{q}_3\end{Bmatrix} = J_q^{-1}J_x\begin{Bmatrix}\dot{x}_P\\ \dot{y}_P\\ \dot{z}_P\end{Bmatrix} \tag{7}$$

while the accelerations from system

$$\begin{Bmatrix}\ddot{q}_1\\ \ddot{q}_2\\ \ddot{q}_3\end{Bmatrix} = J_q^{-1}\left(J_x\begin{Bmatrix}\ddot{x}_P\\ \ddot{y}_P\\ \ddot{z}_P\end{Bmatrix} - \begin{Bmatrix}\dot{x}_P^2+\dot{y}_P^2+(\dot{z}_P-\dot{q}_1)^2\\ \dot{x}_P^2+\dot{y}_P^2+(\dot{z}_P-\dot{q}_2)^2\\ \dot{x}_P^2+\dot{y}_P^2+(\dot{z}_P-\dot{q}_3)^2\end{Bmatrix}\right) \tag{8}$$

## 4 The Lagrangian approach

The generalized coordinate vector is defined as $q = [q_1, q_2, q_3, x_p, y_p, z_p]$. This vector can be partitioned in the vector of the independent parameters $q_1, q_2, q_3$ and the vector of the dependent parameters $x_p, y_p, z_p$: $q = [q_{ind}, q_{dep}]$.

The mass of each cart is $m_{cart}$, the mass of each element between the spherical joints is $m_{link}$ (note that there are 6 of these elements), while the mass of the platform is $m_{plat}$. Fig.2 depicts a simplified lumped mass distribution, in which the mass of each link is splitted in equal parts at the two ends of the link. The extruder nozzle Q is located in point Q at distance PQ below point P. In this work all dissipations are neglected.

The forces $Q_1$, $Q_2$, $Q_3$ on the actuators can be computed from the lagrangian equations (9), valid for j=1 to 6:

$$\frac{d}{dt}\left(\frac{\partial L}{\partial \dot{q}_j}\right) - \frac{\partial L}{\partial q_j} = \sum_{i=1}^{3} \lambda_i \frac{\partial \Gamma_i}{\partial q_j} + Q_j \tag{9}$$

where $\lambda_i$ (i=1 to 3) are the lagrangian multipliers, which can also be computed solving system (9) and $\Gamma_i$ (i=1 to 3) are the closure equations. $Q_j$ are the generalized external forces, assumed to be null on platform: $Q = [Q_1, Q_2, Q_3, 0, 0, 0]$.

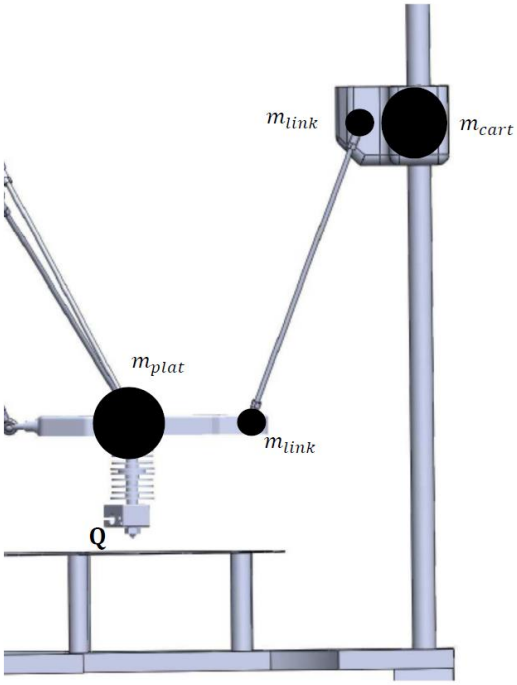


**Fig. 2.** Simplified lumped mass distribution

System (9) can be written in the following matrix form

$$[A]\{x\} = \{b\} \tag{10}$$

where the unknown parameters vector is

$$\{x\} = \{\lambda_1 \quad \lambda_2 \quad \lambda_3 \quad Q_1 \quad Q_2 \quad Q_3\}^T = \begin{Bmatrix}\{\lambda\} \\ \{Q\}\end{Bmatrix} \tag{11}$$

and the constant vector $\{b\}$ involves both inertia terms and the terms due to gravity:

$$\{b\} = [M]\{\ddot{q}\} + \{F\} \tag{12}$$

Partitioning properly system (10), it is possible to obtain the expressions of the lagrangian multipliers and of the actuators forces:

$$\{\lambda\} = \frac{m_{plat} + 3m_{link}}{2}[J_x^T]^{-1}\{\ddot{q}_{dep}\} + \frac{(m_{plat} + 3m_{link})g}{2}[J_x^T]^{-1}\begin{Bmatrix}0\\0\\1\end{Bmatrix} \tag{13}$$

$$\begin{aligned}\{Q\} = (m_{link} + m_{cart})\left(\begin{Bmatrix}\ddot{q}_1\\\ddot{q}_2\\\ddot{q}_3\end{Bmatrix} + g\begin{Bmatrix}1\\1\\1\end{Bmatrix}\right)\\ + (m_{plat} + 3m_{link})[J_q][J_x^T]^{-1}\left(\begin{Bmatrix}\ddot{x}_p\\\ddot{y}_p\\\ddot{z}_p\end{Bmatrix} + g\begin{Bmatrix}0\\0\\1\end{Bmatrix}\right)\end{aligned} \tag{14}$$

### 4.1 Static solution

In case the accelerations are null the static solution is obtained:

$$\{Q\} = (m_{link} + m_{cart})g\begin{Bmatrix}1\\1\\1\end{Bmatrix} + (m_{plat} + 3m_{link})[J_q][J_x^T]^{-1}\, g\begin{Bmatrix}0\\0\\1\end{Bmatrix} \tag{15}$$

In the central position ($x_P$=$y_P$=0) it results

$$\{Q\} = g\begin{Bmatrix}1\\1\\1\end{Bmatrix}\left(2m_{link} + m_{cart} + \frac{m_{plat}}{3}\right) \tag{16}$$

In a not-centered position the actuators forces are different, but their sum results to be

$$\begin{aligned}Q_1 + Q_2 + Q_3 &= 3(m_{link} + m_{cart})g + (m_{plat} + 3m_{link})g\\ &= (6m_{link} + m_{plat} + 3m_{cart})g\end{aligned} \tag{17}$$

which corresponds to the total gravity force of the suspended masses.

## 5 Results and discussion

An example of calculation of actuators forces resulting from given trajectories imposed on the platform is shown in this section. The following masses are considered: $m_{link}$=0.02 kg, $m_{plat}$=0.5 kg and $m_{cart}$=0.25 kg.

The paths are of Lissajous type

$$\boldsymbol{p}(u) = \begin{bmatrix}x_P\\y_P\\z_P\end{bmatrix} = \begin{bmatrix}x_0\sin(\omega_x u + \varphi_x)\\y_0\sin(\omega_y u + \varphi_y)\\PQ\end{bmatrix} \tag{18}$$

with $\omega_x = 6\pi$, $\omega_y = 4\pi$, $\varphi_x = \frac{\pi}{2}$, $\varphi_y = 0$ and 0<$u$<1. Point Q (the extruder nozzle) is supposed to move on the horizontal plane at $z$=0 at constant speed $v$ along the path. The

path has been discretized with a uniform mesh of points corresponding to the position of the end effector at successive time intervals $T_s$. The values $u_k$ are estimated iteratively with the following second order Taylor series, in which vector $\boldsymbol{p}$ denotes the position of the end effector. This equation is valid in case speed $v$ is constant [10]:

$$u_{k+1} = u_k + T_s \frac{v}{\left|\frac{d\boldsymbol{p}}{du}\right|_k} - \frac{T_s^2}{2} v^2 \left[ \frac{\frac{d\boldsymbol{p}^T}{du} \cdot \frac{d^2\boldsymbol{p}}{du^2}}{\left|\frac{d\boldsymbol{p}}{du}\right|^4} \right]_k \tag{19}$$

Fig. 3 illustrates the architecture of the machine, with also the path on the printing bed.

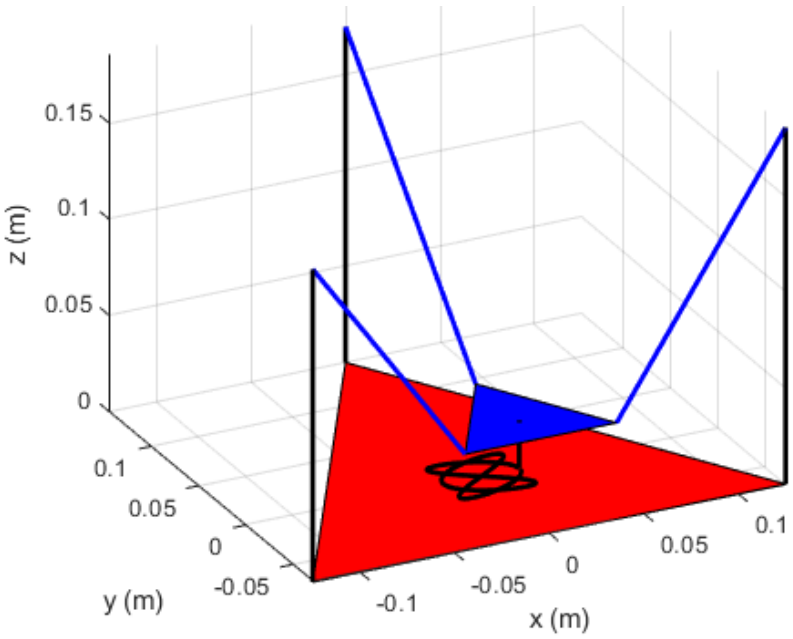


**Fig. 3.** Architecture of the 3D printer

Fig. 4 on top shows force $Q_1$ at different printing speeds (10, 50 and 200 mm/s). It is visible the contribution of inertia forces, which become important increasing speed $v$. It has been verified that the sum of the actuators forces at small speeds coincides with the total gravity force of the suspended masses (about 13.4 N), see fig. 4 at bottom.

In order to further check the results, the time rate of the total energy (potential and kinetic energy) has been compared with the input mechanical power generated by actuators:

$$\frac{d}{dt}(K + U) = Q_1\dot{q}_1 + Q_2\dot{q}_2 + Q_3\dot{q}_3 \tag{20}$$

Fig. 5 compares the two members of Eq. (20), which are found to be coincident, proving the correctness of the results.

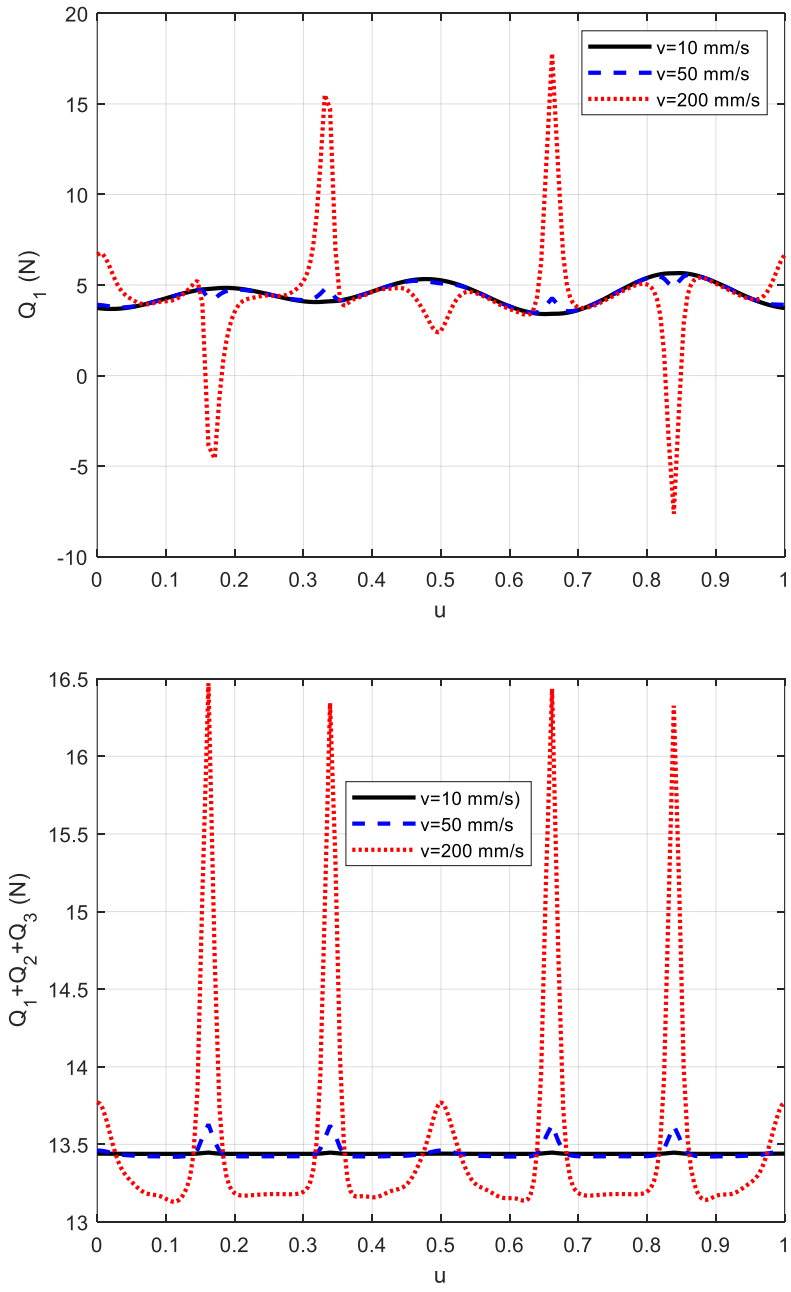


**Fig. 4.** Actuator force $Q_1$ (top) and sum of actuators forces (bottom) at different printing speeds *v*.

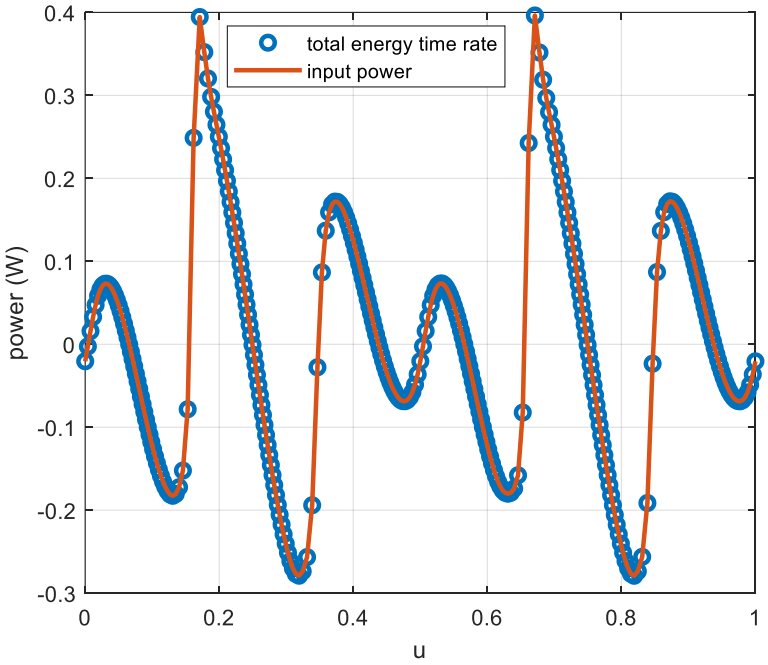


**Fig. 5.** Comparison of the total energy time rate and the input mechanical power with v=200 mm/s

## 6 Conclusions

The direct and inverse kinematics of a delta prismatic robot have been detailed in this paper, together with the dynamic study, carried out with the Lagrangian approach with multipliers. The results have been checked with the principle of energy conservation and checking that at small speeds the total actuators forces coincide with the total weight of the suspended masses. The influence of the inertia forces on the actuators forces is visible increasing the printing speed. The study has carried out in absence of friction and other dissipations for a preliminary set up of the model. Future activity could involve the introduction of dissipative actions in order to have a more realistic model.

## References

1. Clavel, R.: Delta, a fast robot with parallel geometry. In: Proceedings of the 18th International Symposium on Industrial Robots, 91–100. Lausanne, France, 26–28 April 1988.
2. https://reprap.org/wiki/Rostock
3. https://reprap.org/wiki/Kossel

4. López, M., Castillo, E., García, G., & Bashir, A.: Delta robot: Inverse, direct, and intermediate Jacobians. Proceedings of the Institution of Mechanical Engineers, Part C: Journal of Mechanical Engineering Science, 220(1), 103–109 (2006).
5. Zhao, Y.: Singularity, isotropy, and velocity transmission evaluation of a three translational degrees-of-freedom parallel robot. Robotica, 31(2), 193-202 (2013).
6. http://fab.cba.mit.edu/classes/863.15/section.CBA/people/Spielberg/Rostock_Delta_Kinematics_3.pdf
7. Tsai, L.W.: Robot analysis: the mechanics of serial and parallel manipulators. John Wiley & Sons, NY (1999).
8. Staicu, S. and Carp-Ciocardia D. C.: Dynamic analysis of Clavel's Delta parallel robot. In: 2003 IEEE International Conference on Robotics and Automation, (3), 4116-4121. Taipei, Taiwan, (2003).
9. Brinker, J., Corves, B., Wahle, M.: A Comparative Study of Inverse Dynamics based on Clavel's Delta robot. In: The 14th IFToMM World Congress, 89-98, Taipei (Taiwan) (2015).
10. Biagiotti, L. Melchiorri, C.: Trajectory Planning for Automatic Machines and Robots (2010).